PB90-130261

Effect of a Crystal-Melt Interface on Taylor-Vortex Flow

(U.S.) National Inst. of Standards and Technology (NEL)
Gaithersburg, MD

Oct 89

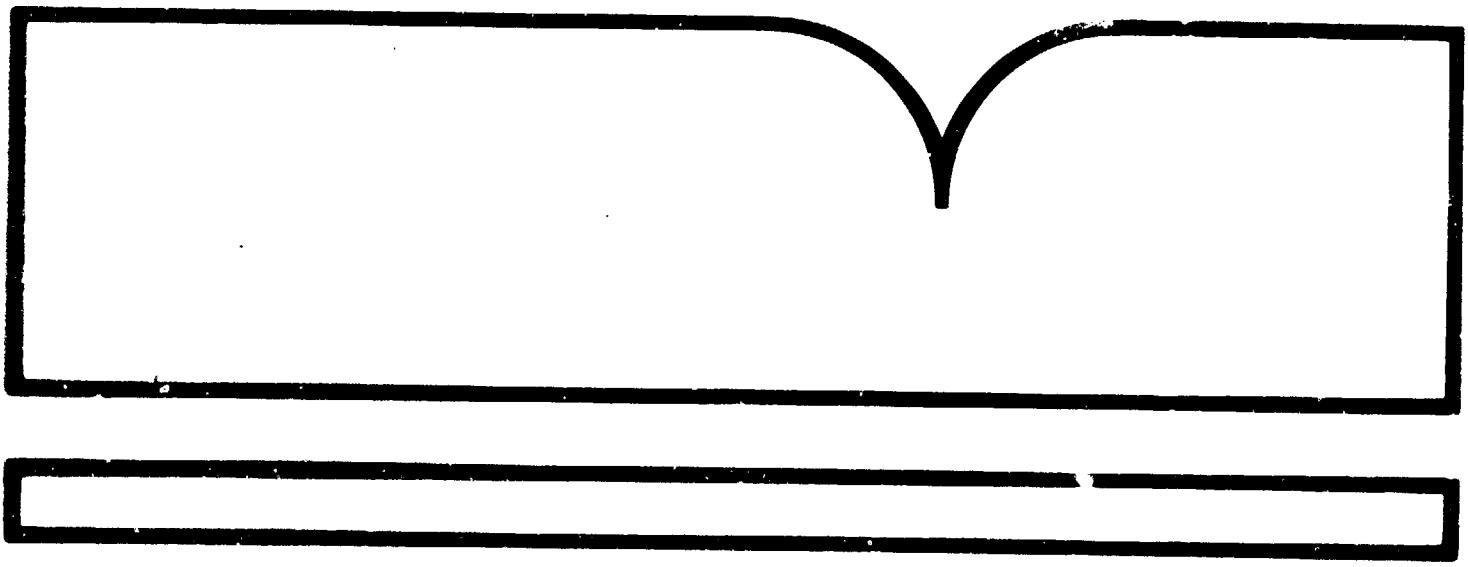

U.S. Department of Commerce
National Technical Information Service
NTIS

PB 90 130261/AS

NIST-114A
(REV. 3-89)

U.S. DEPARTMENT OF COMMERCE
NATIONAL INSTITUTE OF STANDARDS AND TECHNOLOGY

BIBLIOGRAPHIC DATA SHEET

1. PUBLICATION OR REPORT NUMBER
NISTIR 89/4192

2. PERFORMING ORGANIZATION REPORT NUMBER

3. PUBLICATION DATE
OCTOBER 1989

4. TITLE AND SUBTITLE

Effect of a Crystal-Melt Interface on Taylor-Vortex Flow

5. AUTHOR(S)

G. B. McFadden, S. R. Coriell, and B. T. Murray, M. E. Glicksman, M. E. Selleck

6. PERFORMING ORGANIZATION (IF JOINT OR OTHER THAN NIST, SEE INSTRUCTIONS)

U.S. DEPARTMENT OF COMMERCE
NATIONAL INSTITUTE OF STANDARDS AND TECHNOLOGY
GAITHERSBURG, MD 20899

7. CONTRACT/GRANT NUMBER

8. TYPE OF REPORT AND PERIOD COVERED

9. SPONSORING ORGANIZATION NAME AND COMPLETE ADDRESS (STREET, CITY, STATE, ZIP)

NIST Category No.
NIST-340

10. SUPPLEMENTARY NOTES

☐ DOCUMENT DESCRIBES A COMPUTER PROGRAM; SF-185, FIPS SOFTWARE SUMMARY, IS ATTACHED.

11. ABSTRACT (A 200-WORD OR LESS FACTUAL SUMMARY OF MOST SIGNIFICANT INFORMATION. IF DOCUMENT INCLUDES A SIGNIFICANT BIBLIOGRAPHY OR LITERATURE SURVEY, MENTION IT HERE.)

The linear stability of circular Couette flow between concentric infinite cylinders is considered for the case that the stationary outer cylinder is a crystal-melt interface rather than a rigid surface. A radial temperature differnce is maintatined across the iquid gap, and equations for heat transport in the crystal and melt phases are included to extend the ordinary formulation of this problem. The stability of the two-phase system depends on the Prandtl number. For small Prandtl number the linear stability of the two-phase system is given by the classical results for a rigid-walled system. For increasing values of the Prandtl number, convective heat transport becomes significant and the sytem becomes increasingly less stable. Previous results in a narrow-gap approximation are extneded to the case of a finite gap, and both axisymmetric and non-axisymmetric disturbance modes are considered. The two-phase system becomes less stable as the finite gap tends to the narrow-gap limit. The two-phase systen is more stable to non-axisymmetric modes with azimuthal wavenumber n=1; the stability of these n=1 modes is sensitive to the latent heat of fusion.

12. KEY WORDS (6 TO 12 ENTRIES; ALPHABETICAL ORDER; CAPITALIZE ONLY PROPER NAMES; AND SEPARATE KEY WORDS BY SEMICOLONS)

crystal growth, hydrodynamic stability, morphological stability, solidification, taylor-couette flow

13. AVAILABILITY

XX	UNLIMITED
	FOR OFFICIAL DISTRIBUTION. DO NOT RELEASE TO NATIONAL TECHNICAL INFORMATION SERVICE (NTIS).
	ORDER FROM SUPERINTENDENT OF DOCUMENTS, U.S. GOVERNMENT PRINTING OFFICE, WASHINGTON, DC 20402.
XX	ORDER FROM NATIONAL TECHNICAL INFORMATION SERVICE (NTIS), SPRINGFIELD, VA 22161.

14. NUMBER OF PRINTED PAGES
22

15. PRICE

ELECTRONIC FORM

PB90-130261

Applied and
Computational
Mathematics
Division

NISTIR 89-4192

Center for Computing and Applied Mathematics

Effect of a Crystal-Melt Interface on Taylor-Vortex Flow

G.B. McFadden, S.R. Coriell, B.T. Murray, M.E. Glicksman, and M.E. Selleck

October 1989

U.S. DEPARTMENT OF COMMERCE
National Institute of Standards and Technology
Gaithersburg, MD 20899

REPRODUCED BY
U.S. DEPARTMENT OF COMMERCE
NATIONAL TECHNICAL INFORMATION SERVICE
SPRINGFIELD, VA. 22161

Effect of a Crystal-Melt Interface on Taylor-Vortex Flow

G. B. McFadden, S. R. Coriell, and B. T. Murray
National Institute of Standards and Technology
Gaithersburg, Maryland 20899, USA

M. E. Glicksman and M. E. Selleck
Materials Engineering Department
Rennselaer Polytechnic Institute
Troy, New York 12181, USA

Abstract

The linear stability of circular Couette flow between concentric infinite cylinders is considered for the case that the stationary outer cylinder is a crystal-melt interface rather than a rigid surface. A radial temperature difference is maintained across the liquid gap, and equations for heat transport in the crystal and melt phases are included to extend the ordinary formulation of this problem. The stability of this two-phase system depends on the Prandtl number. For small Prandtl number the linear stability of the two-phase system is given by the classical results for a rigid-walled system. For increasing values of the Prandtl number, convective heat transport becomes significant and the system becomes increasingly less stable. Previous results in a narrow-gap approximation are extended to the case of a finite gap, and both axisymmetric and non-axisymmetric disturbance modes are considered. The two-phase system becomes less stable as the finite gap tends to the narrow-gap limit. The two-phase system is more stable to non-axisymmetric modes with azimuthal wavenumber $n = 1$; the stability of these $n = 1$ modes is sensitive to the latent heat of fusion.

1. Introduction

For crystal growth from the melt, the quality of crystal produced depends strongly on the shape of the crystal-melt interface during the growth and on the transport of heat and mass to the interface from the nearby fluid. In particular, instabilities of the interface [1] and hydrodynamic instabilities [2] can promote undesirable inhomogeneities in the growing crystal. Considerable effort goes into the modelling of crystal growth techniques in order to understand and control the process. Since the theoretical problem involves heat and mass transfer via nonlinear convection-diffusion equations in complex geometries, coupled with the free boundary representing the crystal-melt interface, many studies have considered simple geometries for which there are closed-form solutions of the Navier-Stokes equations.

A crystal-melt interface bounding a thermally-supercooled [3] or "constitutionally-supercooled" [4] fluid is subject to *morphological instability* [5], and one line of inquiry is to examine the effect of various types of flow on this interfacial instability [6]. For example, the effect of plane Couette flow [7, 8], rotating disk flow [9], plane stagnation flow [10, 11], thermosolutal convection [12, 13, 14], and the asymptotic suction profile [15], on the instability of a constitutionally-supercooled interface have been investigated. Another possibility is to examine the characteristics of classical hydrodynamic instabilities when a bounding surface is a crystal-melt interface rather than a rigid wall. Such instabilities as Benard convection [16], double-diffusive convection [12, 17, 18], Poiseuille flow [19], the asymptotic suction profile [15], and thermal and shear instabilities in buoyant flow due to lateral heating [19, 20, 21] have all been examined in this light. In general, the problem of predicting the extent of the coupled interaction between the crystal-melt interface and the flow field is not well-understood.

In 1923 G.I. Taylor considered the stability of the steady Couette flow between rotating cylinders and discovered a transition to steady axisymmetric toroidal rolls ("Taylor vortices"), obtaining agreement between the measured val · of the critical rotation rates and his theoretical predictions [23, 24]. If there is a radial temperature difference across the cylindrical gap, the transport of heat is altered by the formation of Taylor vortices, since

convective heat transport then augments the radial diffusive transport. If one of the boundaries is a crystal-melt interface, this change in heat transport can modify the interface shape. More importantly, this change in morphology can alter the conditions for the onset of the Taylor-vortex flow.

In a previous paper we considered the effect of a crystal-melt interface on the Taylor-vortex flow in the narrow-gap approximation [22]. In this note we extend the investigation to include the effects of a finite gap width and non-axisymmetric disturbances.

2. Theory

The geometry is shown in Fig. 1; we consider the linear stability of an idealized system with infinite aspect ratio ($-\infty < z < \infty$ in cylindrical variables). The crystal-melt interface is located at $r = h(z, \phi, t)$, where in the unperturbed base state $h(z, \phi, t) = R_2$ is constant. The heated inner cylinder of radius R_1 rotates at angular velocity Ω_1, setting up a base state consisting of a circular Couette flow in the annular melt occupying the region $R_1 < r < R_2$. The melt is bounded on the outside by a stationary annulus of crystal occupying the region $R_2 < r < R_2 + \bar{L}_S$. Both the heated inner cylinder at $r = R_1$ and the cooling bath at $r = R_2 + \bar{L}_S$ are each assumed to be isothermal, as is the crystal-melt interface, which is at the equilibrium melting temperature. The densities of the melt and crystal are assumed to be the same, and the radial temperature difference across the melt is assumed to be small enough that any buoyancy effects [25] can be neglected.

For details we refer to Ref. [22]. Briefly, the nonlinear governing equations are the incompressible Navier-Stokes equations for the velocity, $\boldsymbol{u}$, and the pressure, p, in the melt region $R_1 < r < h(z, \phi, t)$,

$$\nabla \cdot \boldsymbol{u} = 0, \tag{1a}$$

$$\frac{\partial \boldsymbol{u}}{\partial t} + (\boldsymbol{u} \cdot \nabla)\boldsymbol{u} + \frac{1}{\rho}\nabla p = \nu \nabla^2 \boldsymbol{u}, \tag{1b}$$

and the convection-diffusion equation for the temperature in the melt, T,

$$\frac{\partial T}{\partial t} + (\boldsymbol{u} \cdot \nabla)T = \kappa \nabla^2 T, \tag{2}$$

and the diffusion equation for the temperature in the crystal, T_S,

$$\frac{\partial T_S}{\partial t} = \kappa_S \nabla^2 T_S. \tag{3}$$

Here ρ is the density, ν is the kinematic viscosity, and κ and κ_S are the thermal diffusivities of the melt and crystal, respectively. At the crystal-melt interface $r = h(z, \phi, t)$ and the inner cylinder $r = R_1$ the flow satisfies no slip and no normal flow, $\boldsymbol{u} = 0$. The temperatures are specified at the inner cylinder and the outer edge of the crystal. The thermal boundary conditions at the interface are

$$k\frac{\partial T}{\partial n} - k_S\frac{\partial T_S}{\partial n} = -L_V v_n \tag{4a}$$

$$T = T_S = T_m + T_m \Gamma \mathcal{K}, \tag{4b}$$

where $\partial/\partial n$ is the normal derivative, k and k_S are the thermal conductivities of the liquid and crystal, respectively, T_m is the bulk melting point of the crystal, L_V is the latent heat of fusion per unit volume of crystal, v_n is the normal velocity of the interface, and Γ is a capillary length. Eq. (4a) expresses the conservation of energy: the latent heat released by the phase transition is conducted into the crystal and melt. Eq. (4b) is the Gibbs-Thomson equation which relates the interface temperature to the mean curvature of the interface, $\mathcal{K}$.

We consider the stability of the one-dimensional base state given by $h(z, \phi, t) = R_2$, $u = w = 0$, $v = V^{(0)}(r)$, $p = p^{(0)}(r)$, $T = T^{(0)}(r)$, and $T_S = T_S^{(0)}(r)$, where u, v, and w are the radial, azimuthal, and axial velocity components, respectively,

$$V^{(0)}(r) = r\Omega_1 \frac{(R_2^2/r^2 - 1)}{(R_2^2/R_1^2 - 1)} \tag{5}$$

$$T^{(0)}(r) = T_m + T_m\frac{\Gamma}{R_2} + \Delta T \frac{\log(r/R_2)}{\log(R_1/R_2)}, \tag{6}$$

and

$$T_S^{(0)}(r) = T_m + T_m\frac{\Gamma}{R_2} + \left(\frac{k}{k_S}\right)\Delta T \frac{\log(r/R_2)}{\log(R_1/R_2)}; \tag{7}$$

the base pressure gradient balances the centripetal acceleration term $\rho(V^{(0)})^2/r$.

To determine the linear stability of the base state, we assume the dependence of the perturbed quantities takes the form $f(r)\exp(\sigma t + in\phi + iaz)$, and write

$$\begin{pmatrix} u \\ v \\ w \\ p \\ T \\ T_S \\ h \end{pmatrix} = \begin{pmatrix} 0 \\ V^{(0)}(r) \\ 0 \\ p^{(0)}(r) \\ T^{(0)}(r) \\ T_S^{(0)}(r) \\ R_2 \end{pmatrix} + \begin{pmatrix} \hat{u}(r) \\ \hat{v}(r) \\ \hat{w}(r) \\ \hat{p}(r) \\ \hat{T}(r) \\ \hat{T}_S(r) \\ \hat{\delta} \end{pmatrix} \exp(\sigma t + in\phi + iaz), \tag{8}$$

where the small quantities $\hat{u}$, $\hat{v}$, $\hat{w}$, $\hat{p}$, $\hat{T}$, $\hat{T}_S$ and $\hat{\delta}$ are complex. The exponential growth rate σ is complex as well, and the base state is linearly stable if σ_r, the real part of σ, is negative for all wavenumbers a and n. A marginal disturbance ($\sigma_r = 0$) is stationary if σ_i, the imaginary part of σ, vanishes.

The equations and boundary conditions are linearized about the base state and the resulting eigenvalue problem describing the linear stability of the system is solved numerically using the same approach described in [22]. The dimensionless parameters which enter the problem are the Taylor number

$$T_a = \frac{4[R_2 - R_1]^2 R_1^2 \Omega_1^2}{\nu^2},$$

the Prandtl number $P_r = \nu/\kappa$, the ratio $P_S = \nu/\kappa_S$, the dimensionless latent heat of fusion $\mathcal{L} = \nu L_V/(k\Delta T)$, the dimensionless surface energy $\gamma = T_m\Gamma/([R_2 - R_1]\Delta T)$, the ratio of thermal conductivities $q = k_S/k$, the radius ratio $\eta = R_1/R_2$, and the dimensionless crystal width $L_c = \bar{L}_S/[R_2 - R_1]$.

3. Numerical Results

Our principal concern is the interpretation of recent experiments with succinonitrile (SCN) with $P_r = 22.8$, for the case of a finite gap $\eta < 1$. For centimeter-sized systems with

moderate temperature differences across the melt gap, the parameter γ is very small and can be neglected. The thermal properties of the crystal and melt are very similar for SCN, and we will take $q = 1$ and $P_S = 22.8$. We take $L_c = 1$; the effect of varying L_c is considered in Ref. [22] for the narrow gap limit. We will present our numerical results in dimensionless form, using the length scale $[R_2 - R_1]$, the time scale $[R_2 - R_1]^2/\nu$, the temperature scale ΔT, and the fluid velocity scale $\Omega_1[R_2 - R_1]$. However, we will retain the previous notation for all quantities, which will henceforth be dimensionless.

3.1. Axisymmetric modes

For axisymmetric disturbances to the two-phase system we find that, as in the rigid-walled system, the onset of instability is stationary, with $\sigma_i = 0$. In this case the marginal Taylor numbers do not depend on $\mathcal{L}$, P_S, or q. In Fig. 2 we show marginal stability curves for a fixed radius ratio $\eta = 0.5$ for various values of the Prandtl number. For $P_r = 0$ the thermal transport is diffusion-controlled and convection has no effect on the thermal field. The isotherms, and hence the crystal-melt interface, are therefore cylindrical, as dictated by the isothermal boundary conditions at $r = R_1$ and $r = R_2 + L$. The results for $P_r = 0$ therefore are identical to the results for a rigid-walled system, with a critical Taylor number $T_a = 6,200$ corresponding to a dimensionless wavenumber $a = 3.2$. As P_r increases, convective transport of heat becomes significant, and the interface responds to the influence of the flow field, which allows the instability to set in sooner: for $P_r = 22.8$, the critical disturbance has $T_a = 1,060$ and $a = 1.7$.

In Figs. 3 and 4 we show the linear eigenmodes for $P_r = 0.01$ and $P_r = 22.8$ in detail, together with contour plots of the flow field and temperature in the melt. On the left of each plot we show the dimensionless angular velocity of the base state $\Omega(r) = V^{(0)}(r)/r$, and the dimensionless eigenfunctions $\hat{u}(r)$, $\hat{v}(r)$, and $\hat{T}(r)$, normalized so that the maximum value of $\hat{u}$ is one. The contour plots show a cross-section of the melt and crystal, with the cross-hatched region corresponding to the crystal; the plots are obtained by adding to the base state a small multiple (0.003) of the normalized eigenmode, in order to highlight the

interface deformation. For $P_r = 0.01$ with $a = 3.162$ the effect of the crystal-melt interface on the classical Taylor-vortex flow is small, and the flow consists of counter-rotating cells of roughly unit aspect ratio. The isotherms are undisturbed by the flow, and show the logarithmic spacing of the base state. For $P_r = 22.8$ with $a = 1.697$ (Fig. 4) the perturbed azimuthal velocity and temperature fields are larger, and the interface and isotherms are distorted by the flow field. The counter-rotating cells have a rectangular cross-section. The interface melts back where the perturbed flow transports additional heat to the interface, and protrudes into the liquid where the flow carries heat away from the interface. Note also that $\hat{v}$ is much larger near the interface for $P_r = 22.8$ than it is in the rigid case for $P_r = 0$.

In Fig. 5 we show marginal stability curves for $P_r = 22.8$ for various values of the radius ratio η. As is the case for the rigid-walled system, the effect of decreasing η from the narrow-gap limit $\eta = 1$ is to stabilize the system. As can be seen from Table I, the amount of destabilization relative to the rigid-walled system remains about the same over this range of η, amounting to a five-fold to seven-fold decrease in the critical Taylor number; the critical wavenumber is not sensitive to η over this range.

3.2. Non-axisymmetric modes

We next consider the behavior of non-axisymmetric disturbances with $n \neq 0$. For a rigid-walled system in the narrow gap limit, the most dangerous mode is axisymmetric, but there are also nearby non-axisymmetric modes at only slightly higher Taylor numbers [26]. In contrast to the axisymmetric case, which has a stationary onset of instability ($\sigma_i = 0$), the non-axisymmetric modes have non-zero values of σ_i, and the disturbance propagates as a travelling wave. Thus, whereas the critical Taylor number for the axisymmetric mode is insensitive to the latent heat in the two-phase problem, for the non-axisymmetric mode energy must be continually supplied locally to transform crystal to melt to sustain the progressing wave. Consequently the critical Taylor numbers for the non-axisymmetric modes are found to depend on the value of the latent heat.

The dimensionless parameter $\mathcal{L} = \nu L v/(k\Delta T)$ is a measure of the amount of energy

required to transform crystal into melt. Either a small value of the latent heat L_V or a large temperature difference ΔT across the melt give rise to a small value of $\mathcal{L}$, meaning that it is relatively easy to melt the crystal. If the latent heat is large, or the temperature difference across the melt is small, it is difficult to provide enough heat to melt the crystal. Evaluating the material constants for SCN, the dimensionless latent heat can be written in the form $\mathcal{L} = 557.3/\Delta T$, for ΔT given in Kelvins. As shown in Fig. 6 for $\eta = 0.99$, for $n = 1$ modes the two-phase system is least stable for $\mathcal{L} = 0$, becoming more stable with increasing $\mathcal{L}$. The marginal Taylor number for the $n = 1$ modes for $\mathcal{L} = 0$ is $T_a = 1150$, which is significantly higher than the $n = 0$ value, $T_a = 670$. As T_a is increased, the neutral stability curves begins to pinch off, as shown for $\mathcal{L} = 50$, and eventually forms two branches, as shown for $\mathcal{L} = 350$. The upper of the two branches tends to the marginal curve corresponding to the rigid-walled system for large values of $\mathcal{L}$, and the interface deflection for the normalized eigenmode tends to zero as $\mathcal{L}^{-1}$. The interface deflection for modes on the lower closed loop of marginal states tends to a non-zero limit for large $\mathcal{L}$, and the product $\mathcal{L}\sigma_i$ tends to a constant. We have not investigated further the nature of this lower branch, as in any event the most dangerous mode for the two-phase system corresponds to an axisymmetric mode for these parameter values.

For non-axisymmetric modes, then, the destabilizing effect of convective heat transport to the interface at large Prandtl number can be somewhat offset by large values of $\mathcal{L}$. In Table II we compare the marginal Taylor numbers for $n = 0$ and $n = 1$ modes in the rigid-walled system ($P_r = 0$) and the two-phase system ($P_r = 22.8$) for radius ratios η near unity. The comparison is made with $\mathcal{L} = 0$, which is the *least* stable case for the $n = 1$ mode. For $P_r = 22.8$, the $n = 1$ mode is substantially more stable than the $n = 0$ mode, unlike the rigid-walled case. The $n = 1$ mode is also much more stabilized for decreasing η than are the other modes in the systems.

4. Discussion

The destabilization of the two-phase system relative to the rigid-walled system for large Prandtl numbers that was found for the case of a narrow gap [22] also occurs for a finite gap system, although the relative destabilization is largest for the narrow gap case. As for the case of a rigid-walled system, for steady rotation of the inner cylinder with a stationary outer cylinder, the onset of instability is due to a stationary, axisymmetric mode. The non-axisymmetric modes with azimuthal wavenumber $n = 1$ that are nearby the onset for the rigid-walled system are found to be relatively more stable for the two-phase system.

A possible extension of this work would include the effects of buoyancy-driven flow caused by the radial temperature gradient in a vertical alignment of the system. As in the rigid-walled case [27], a one-dimensional solution may be found for the limiting case of an infinite aspect ratio, and a tractable linear stability problem may be formulated.

It is also of interest to consider the case of a time-varying torsional oscillation of the system with zero mean oscillation, and preliminary experimental and theoretical work on this problem is in progress; the theoretical treatment is based on Floquet theory. Preliminary experimental results for the two-phase system using succinonitrile [22] suggest an axisymmetric mode of instability, whereas the numerical results of Carmi and Tustaniwskyj [28] for an oscillating rigid-walled system indicate a non-axisymmetric (n = 1) mode of instability, with nearby axisymmtric modes that are only slightly more stable.

5. Acknowledgements

The research was supported by the Microgravity Sciences and Applications Program, NASA, and the Applied Mathematics Program of the Defense Advanced Research Projects Agency. The third author (BTM) was supported by an National Research Council Postdoctoral Research Fellowship.

References

[1] S. R. Coriell, G. B. McFadden & R. F. Sekerka, Ann. Rev. Mater. Sci. **15**, 119 (1985).

[2] M. E. Glicksman, S. R. Coriell & G. B. McFadden, Ann. Rev. Fluid Mech. **18**, 307 (1986).

[3] S. C. Hardy & S. R. Coriell, *J. Crystal Growth* **5**, 329 (1969).

[4] W. A. Tiller, J. W. Rutter, K. A. Jackson & B. Chalmers, Acta Metall. **1**, 428 (1953).

[5] W. W. Mullins & R. F. Sekerka, J. Appl. Phys. **35**, 444 (1964).

[6] S. R. Coriell & R. F. Sekerka, PhysicoChem. Hydrodyn. **2**, 281 (1981).

[7] R. T. Delves, in *Crystal Growth*, edited by B. R. Pamplin (Pergamon, New York, 1974), vol. 6, p. 40.

[8] S. R. Coriell, G. B. McFadden, R. F. Boisvert & R. F. Sekerka, J. Crystal Growth **69**, 15 (1984).

[9] K. Brattkus & S. H. Davis, J. Crystal Growth **87**, 385 (1988).

[10] K. Brattkus & S. H. Davis, J. Crystal Growth **89**, 423 1988.

[11] G. B. McFadden, S. R. Coriell, & J. Iwan D. Alexander, Comm. Pure Appl. Math. **16**, 683 (1988).

[12] S. R. Coriell, M. R. Cordes, W. J. Boettinger & R. F. Sekerka, J. Crystal Growth **49**, 13 (1980).

[13] G. W. Young & S. H. Davis, Phys. Rev. **B34**, 3388 (1986).

[14] S. R. Coriell & G. B. McFadden, J. Crystal Growth **94**, 513 (1989).

[15] S. A. Forth & A. A. Wheeler, J. Fluid Mech. **202**, 339 (1989).

[16] S. H. Davis, U. Muller & C. Dietsche, J. Fluid Mech. **144**, 133 (1984).

[17] D. R. Jenkins, IMA J. Appl. Math. **35**, 145 (1985).

[18] B. Caroli, C. Caroli, C. Misbah & B. Roulet, J. Physique **46**, 401 (1985).

[19] G. B. McFadden, S. R. Coriell, R. F. Boisvert, M. E. Glicksman & Q. T. Fang, Metal. Trans. **15A**, 2117 (1984).

[20] S. R. Coriell, G. B. McFadden, R. F. Boisvert, M. E. Glicksman & Q. T. Fang, J. Crystal Growth **66**, 514 (1984).

[21] Q. T. Fang, M. E. Glicksman, S. R. Coriell, G. B. McFadden & R. F. Boisvert, J. Fluid Mech. **151**, 121 (1985).

[22] G. B. McFadden, S. R. Coriell, M. E. Glicksman, & M. E. Selleck. Instability of a Taylor-Couette flow interacting with a crystal-melt interface. PhysicoChem. Hydrodyn., in press (1989).

[23] G. I. Taylor, Phil. Trans. Roy. Soc. A **223**, 289 (1923).

[24] P. G. Drazin & W. H. Reid, *Hydrodynamic Stability.* (Cambridge University Press, Cambridge, 1981).

[25] H. A. Snyder, Ann. Phys. **31**, 292 (1965).

[26] E. R. Krueger, A. Gross & R. C. DiPrima, J. Fluid Mech. **24**, 521 (1966).

[27] M. E. Ali, The stability of Taylor-Couette flow with radial heating. Ph. D. Dissertation, Dept. of Mech. Eng., University of Colorado, Boulder, Colorado, 1988.

[28] S. Carmi & J. I. Tustaniwskyj, J. Fluid Mech. **108**, 19 (1981).

Table I. Comparison of Rigid and Two-Phase Systems

P_r	$\eta = 0.99$		$\eta = 0.50$		$\eta = 0.30$		$\eta = 0.20$	
	T_a	a	T_a	a	T_a	a	T_a	a
0.0	3,412.63	3.127	6,199.16	3.162	11,548.16	3.215	20,715.77	3.263
22.8	670.14	1.749	1,059.17	1.697	1,834.04	1.671	3,144.69	1.652

Table II. Comparison of Axisymmetric and Non-Axisymmetric Modes

P_r		$\eta = 0.99$		$\eta = 0.97$		$\eta = 0.95$	
		$n = 0$	$n = 1$	$n = 0$	$n = 1$	$n = 0$	$n = 1$
0.0	T_a	3,412.63	3,416.93	3,459.89	3,473.51	3,509.71	3,533.70
	a	3.127	3.128	3.127	3.131	3.127	3.135
	σ_i	0.0	-2.180	0.0	-3.828	0.0	-5.009
22.8	T_a	670.14	1,150.46	676.07	1,692.84	682.39	2,081.06
	a	1.749	2.322	1.747	2.636	1.746	2.787
	σ_i	0.0	-0.398	0.0	-0.819	0.0	-1.236

Figure Captions

Figure 1. Schematic of the case of a stationary crystalline annulus (c) surrounding an annular melt (ℓ) in contact with an inner cylinder rotating at angular velocity Ω_1.

Figure 2. Marginal Taylor numbers versus the axial wavenumber a for axisymmetric modes with Prandtl numbers $P_r = 0.0$, 5.0, 22.8, and 100.0.

Figure 3. The linear eigenmode for $P_r = 0.01$ and $\eta = 0.5$. $\Omega(r)$, $\hat{u}(r)$, $\hat{v}(r)$, and $\hat{T}(r)$ are the dimensionless angular velocity of the base state, the radial part of the perturbed dimensionless radial velocity, the radial part of the perturbed dimensionless azimuthal velocity, and the radial part of the perturbed dimensionless temperature in the melt, respectively. Streamlines of the flow are shown in the contour plot in the middle, with the cross-hatched region corresponding to the crystal. Isotherms are shown in the contour plot on the right.

Figure 4. The linear eigenmode for $P_r = 22.8$ and $\eta = 0.5$. As in Figure 3, in the contour plots the linear perturbation, normalized so that $\max\{\tilde{u}(r)\} = 1$, is added to the base state with an amplitude of 0.003 to show the interface deformation.

Figure 5. Marginal Taylor numbers for axisymmetric modes with $P_r = 22.8$, versus the axial wavenumber a for radius ratios $\eta = R_1/R_2$ of 0.990, 0.50, 0.30, and 0.20.

Figure 6. Marginal Taylor numbers for non-axisymmetric modes, versus the axial wavenumber a for values of the dimensionless latent heat $\mathcal{L} = 0$, 50, and 350. There are two branches of the marginal stability curve for $\mathcal{L} = 350$; the upper branch is nearly identical to that for the rigid-walled system.

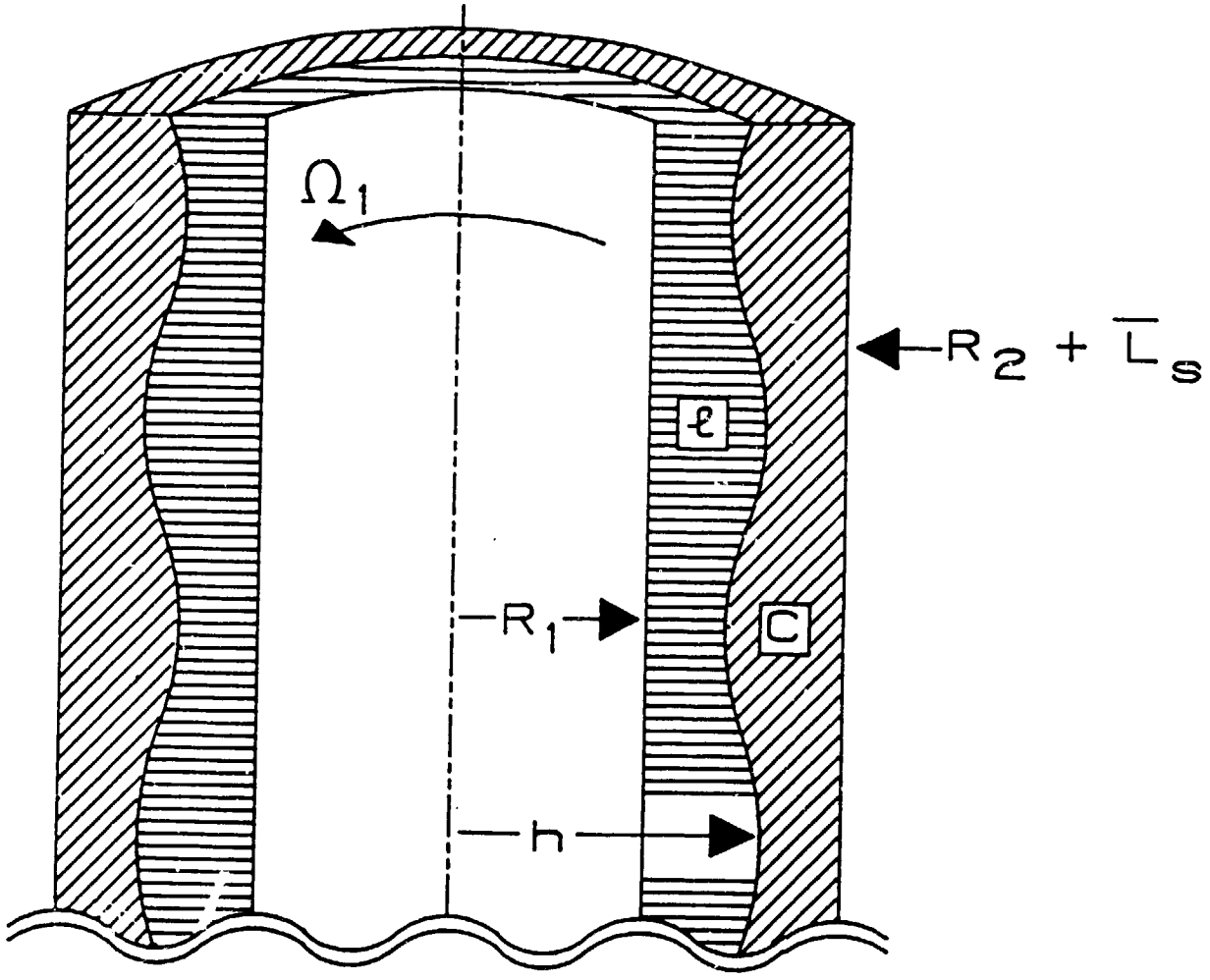

Figure 1

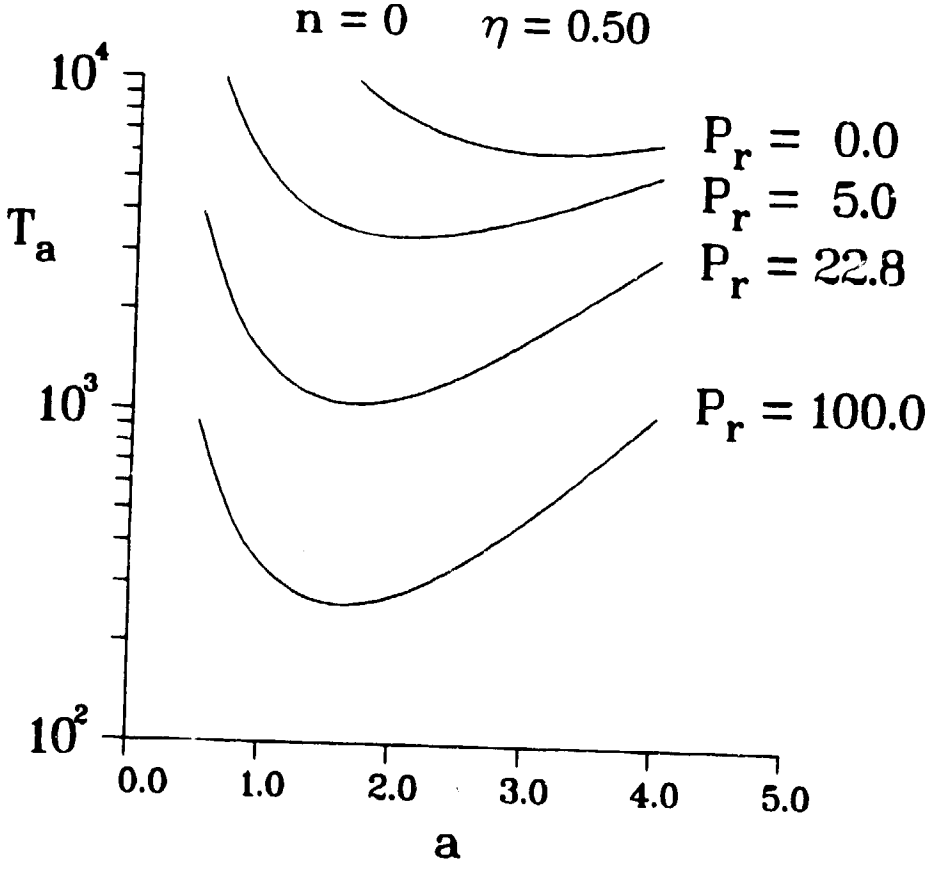
n = 0
$\eta = 0.50$
10^4
10^3
10^2
T_a
$P_r = 0.0$
$P_r = 5.0$
$P_r = 22.8$
$P_r = 100.0$
0.0
1.0
2.0
3.0
4.0
5.0
a

Figure 2

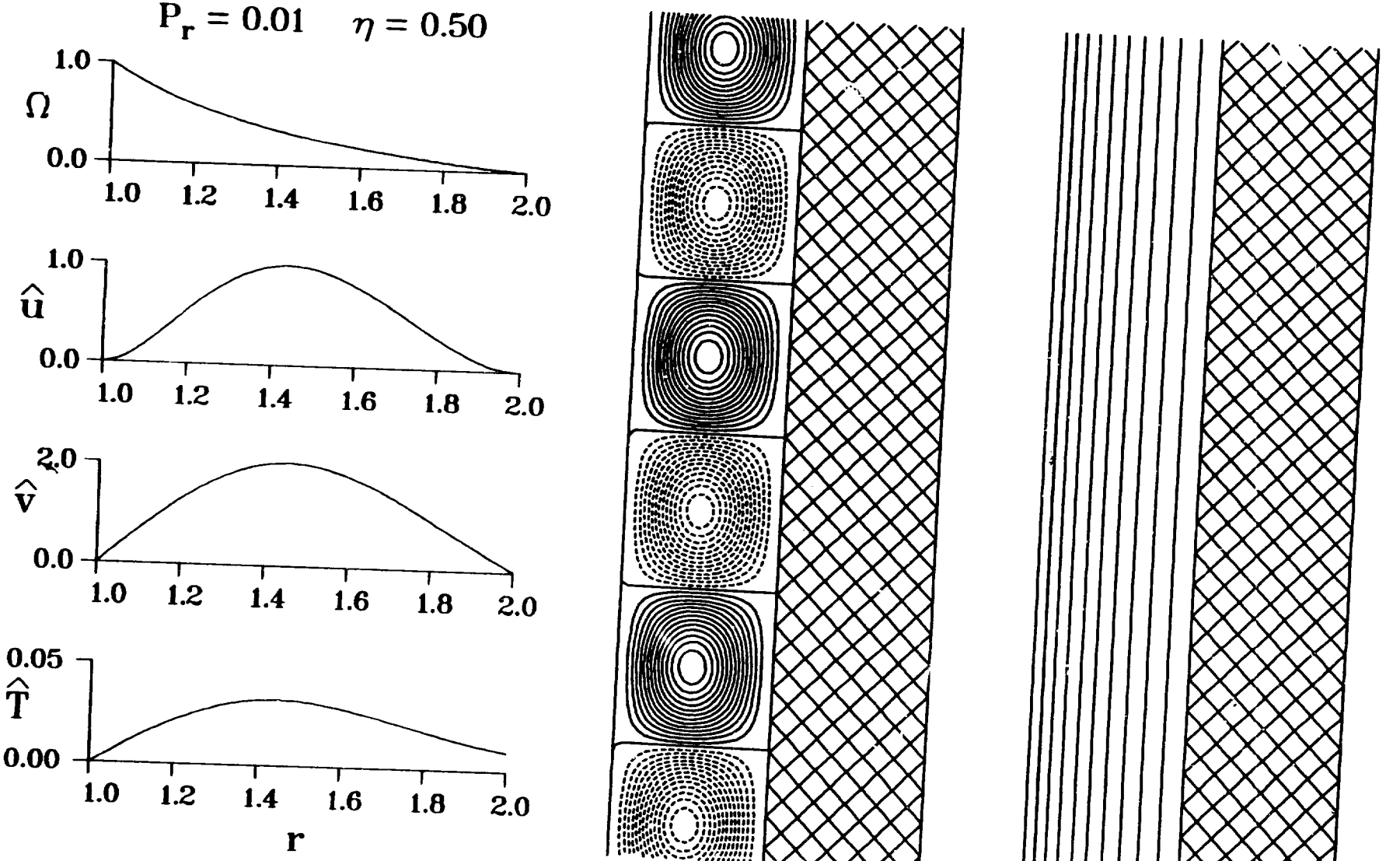
$P_r = 0.01$ $\eta = 0.50$
1.0
Ω
0.0
1.0 1.2 1.4 1.6 1.8 2.0
1.0
$\hat{u}$
0.0
1.0 1.2 1.4 1.6 1.8 2.0
2.0
$\hat{v}$
0.0
1.0 1.2 1.4 1.6 1.8 2.0
0.05
$\hat{T}$
0.00
1.0 1.2 1.4 1.6 1.8 2.0
r

Figure 3

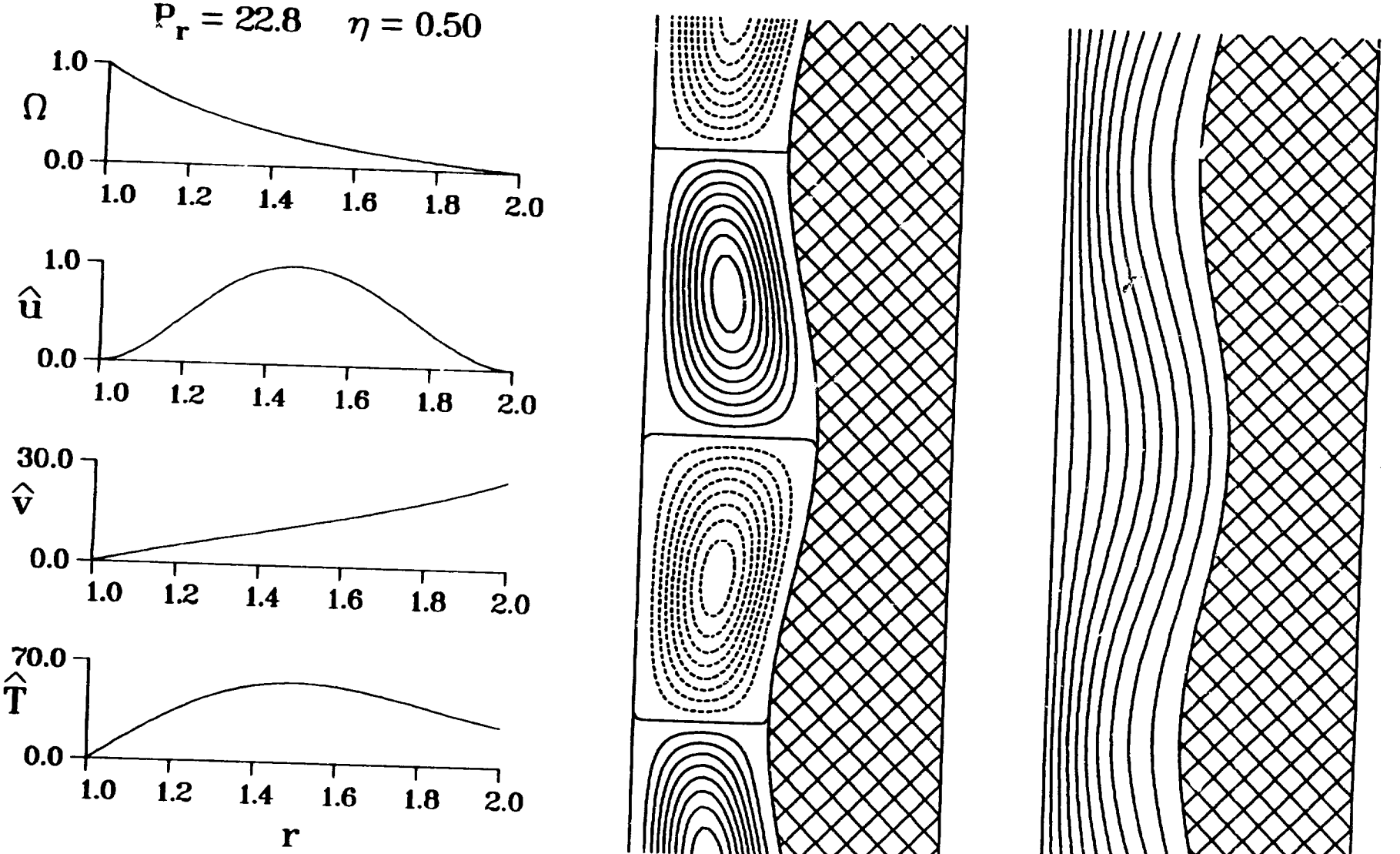
$P_r = 22.8$ $\eta = 0.50$
1.0
Ω
0.0
1.0 1.2 1.4 1.6 1.8 2.0
1.0
$\hat{u}$
0.0
1.0 1.2 1.4 1.6 1.8 2.0
30.0
$\hat{v}$
0.0
1.0 1.2 1.4 1.6 1.8 2.0
70.0
$\hat{T}$
0.0
1.0 1.2 1.4 1.6 1.8 2.0
r

Figure 4

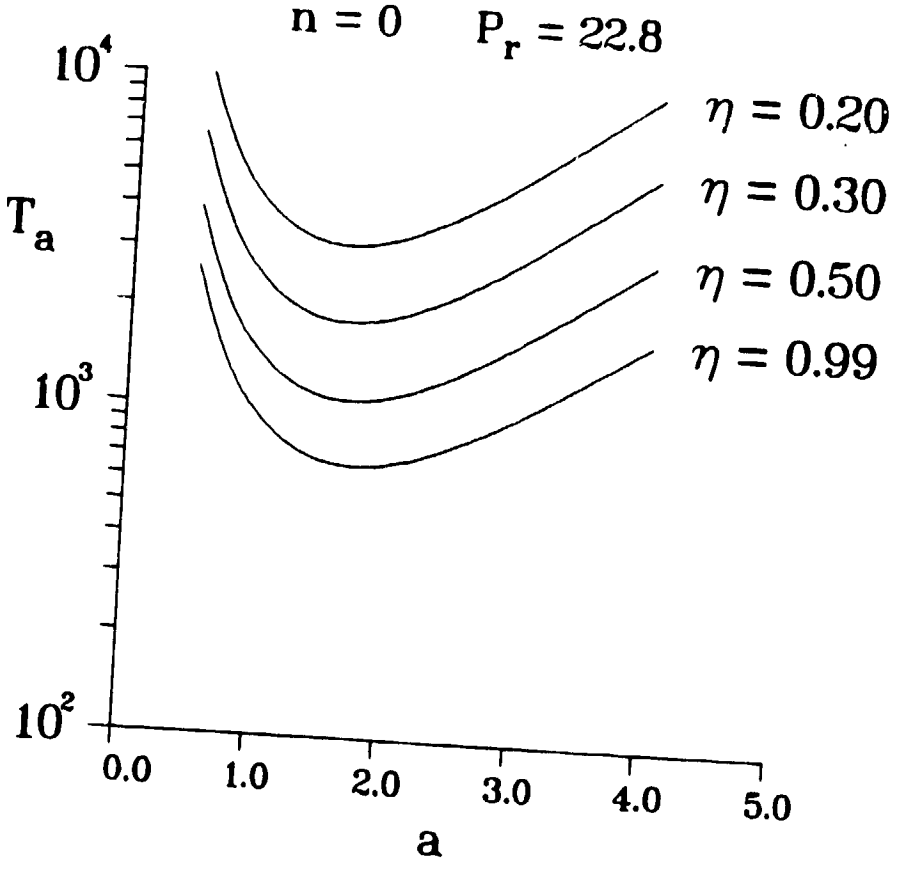
n = 0
$P_r = 22.8$
10^4
T_a
10^3
10^2
$\eta = 0.20$
$\eta = 0.30$
$\eta = 0.50$
$\eta = 0.99$
0.0
1.0
2.0
3.0
4.0
5.0
a

Figure 5

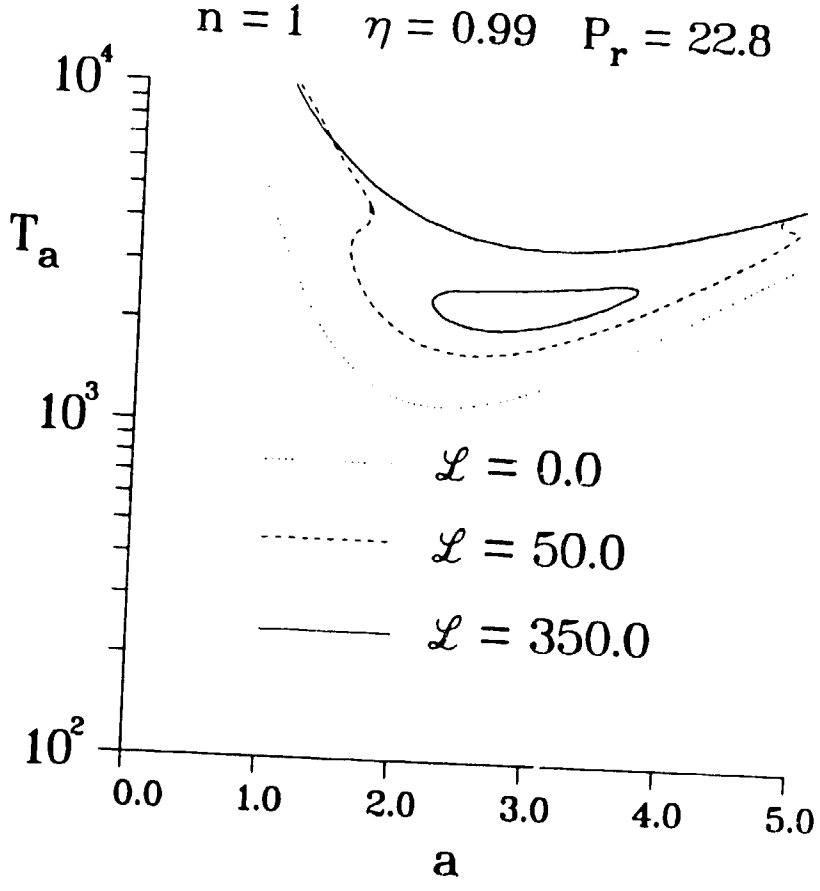
n = 1 η = 0.99 P_r = 22.8
10^4
T_a
10^3
10^2
$\mathcal{L}$ = 0.0
$\mathcal{L}$ = 50.0
$\mathcal{L}$ = 350.0
0.0
1.0
2.0
3.0
4.0
5.0
a

Figure 6